

2-9-1993

## Evaluation of the Surface Roughness of Cystine Stones Using a Visible Laser Diode Scattering Approach

R. Thibert  
*Université de Montréal*

B. Dubuc  
*McGill University*

M. Dofour  
*National Research Council of Canada*

R. Tawashi  
*Université de Montréal*

Follow this and additional works at: <https://digitalcommons.usu.edu/microscopy>

 Part of the [Biology Commons](#)

---

### Recommended Citation

Thibert, R.; Dubuc, B.; Dofour, M.; and Tawashi, R. (1993) "Evaluation of the Surface Roughness of Cystine Stones Using a Visible Laser Diode Scattering Approach," *Scanning Microscopy*: Vol. 7 : No. 2 , Article 12. Available at: <https://digitalcommons.usu.edu/microscopy/vol7/iss2/12>

This Article is brought to you for free and open access by the Western Dairy Center at DigitalCommons@USU. It has been accepted for inclusion in Scanning Microscopy by an authorized administrator of DigitalCommons@USU. For more information, please contact [digitalcommons@usu.edu](mailto:digitalcommons@usu.edu).



## EVALUATION OF THE SURFACE ROUGHNESS OF CYSTINE STONES USING A VISIBLE LASER DIODE SCATTERING APPROACH

R. Thibert<sup>1</sup>, B. Dubuc<sup>2</sup>, M. Dufour<sup>3</sup>, R. Tawashi<sup>1\*</sup>

<sup>1</sup>Faculté de Pharmacie, Université de Montréal, Montréal, Canada

<sup>2</sup>Department of Electrical Engineering, McGill University, Montréal, Canada

<sup>3</sup>Industrial Materials Institute, National Research Council of Canada, Boucherville, Canada

(Received for publication June 23, 1992, and in revised form February 9, 1993)

### Abstract

To understand the processes of fragmentation and the chemical reactivity of solids, proper characterization of surface topography is crucial. This paper describes a non-destructive technique of quantifying the surface roughness of cystine renal stones, using visible laser diode scattering and fractal geometry. Fragments of cystine stones were mounted on microscope slides and coated by a carbon-sputtering apparatus. The slides were placed under a dynamic active-vision system, using a visible laser diode to measure three-dimensional surface coordinates. The data obtained were analyzed by fractal geometry. Surface fractal dimensions were determined by the variation method. The results showed that the surface of a compact-size sample can be evaluated quantitatively. The technique is valuable for the accurate presentation of surfaces in three dimensions.

### Introduction

The surface aspects of solids are of great importance in wettability, dissolution, adsorption, mixing, catalysis and chemical reactivity. An adequate and precise method of quantification of surface topography is needed to better understand physicochemical processes at the interface. The limits of accuracy of a given method should be selected according to the ultimate application desired and relevance to the process under investigation.

The importance of surfaces and surface roughness has been recognized in different fields. Pharmaceutical technology has established measurement of the surface roughness of tablets (Hess, 1978), the relation between surface roughness and adhesion of film coating (Rowe, 1978; Trudelle et al., 1988), and surface roughness effects on the surface wettability of polymer films and compressed disks (Zografi and Johnson, 1984). Recent surface roughness studies have focused on the potential implications of surface and interfacial geometries in heterogeneous reactions (Avnir and Farin, 1990). In the biomedical field, surface aspects have started to receive special attention. For example, contact lenses manufactured by certain processes may represent an increased risk of conjunctival damage (Fowler and Gaertner, 1990).

The microstructure of surfaces can vary on all length scales, from the atomic up to the macroscopic scale. Surface defects at the atomic level, for example, may interact with functional groups of higher proteins. At the macroscopic end, surface irregularities may influence cell behavior (Brunette, 1988). Merritt and Chang (1991) recently defined a series of factors that influence bacterial adherence to biomaterials and suggested that detailed procedures should be implemented to standardize methods used to study adherence phenomena as a function of surface characteristics.

There is no simple, flexible, and non-destructive method for evaluating surface roughness. Most studies reported so far have mainly provided a qualitative or semi-quantitative appreciation of surface irregularity. In previous work, we demonstrated the use of perimeter

Key Words: Cystine renal stone, fractal analysis, laser diode scattering, surface roughness.

\*Address for correspondence:

Rashad Tawashi

Université de Montréal, Faculté de Pharmacie  
Montréal (Québec), Canada H3C 3J7

Phone No.: (514) 343-6455

FAX No.: (514) 343-2102

fractal dimension in the investigation of surface geometry during renal stone fragmentation (Thibert and Tawashi, 1991). The main objective of the present experiment was to describe a method that can quantitatively evaluate surface roughness in three dimensions.

#### Materials and Methods

In this work, renal cystine stone fragments were chosen as a model for the quantitative assessment of surface ruggedness. Cystine renal stones were classified recently as either rough or smooth and this qualitative classification was correlated to their fragmentability or ease of stone fragmentation using extracorporeal shock wave lithotripsy (Bhatta et al., 1989). Samples of fragments 6-8 mm in diameter were obtained from the Royal Victoria Hospital and Louis C. Herring & Co. after shock wave lithotripsy or removal by surgery. The fragments were mounted on microscope slides with epoxy having a 5 minute curing time. The original external surface was coated with a layer of approximately 100 Å of carbon and examined by scanning electron microscopy (Jeol, JSM 820). Fragments were selected to represent both "smooth" and "rough" stones as described by Bhatta et al. (1989).

In this report the term "roughness" is used to characterize the macrotecture of the surface (i.e. the organisation of features at a large scale: 100-1000  $\mu\text{m}$ ) rather than the microtexture (features in the order of 10  $\mu\text{m}$ ), even if in some cases the two types of textures coexist. This scale range was chosen because it is appropriate for the study of stone fragmentation. The size of the studied features makes the use of a contact stylus profilometer impossible, therefore justifying the use of a triangulation sensing technique.

#### Data acquisition

For surface analysis, the slides were placed under a dynamic active-vision system, using a visible laser diode to measure 3-D surface coordinates. This system is composed of a visible laser diode (Toshiba, TOLD9215), a CCD camera (Panasonic, WV-CD50) and a moving stage (Micro-Contrôle, MT-160) which are linked to a personal computer. Specially developed software gives access to image acquisition and image reconstruction for 3-D rendering. The optical axes of the laser and camera are at an angle ( $\theta = 45^\circ$ ) for triangulation to obtain 3-D coordinates (Dickson and Harkness, 1969; Dufour and Bégin, 1984). As seen in Figure 1, point  $A$  is imaged on the detector plane of the camera by the laser source placed at an angle of  $45^\circ$ . If the position of the image point changes from  $A$  to  $A'$ , its image will move from  $O$  to  $O'$ . Using the law of sines, we write:

$$d = \frac{OO'}{m \sin \theta} \quad (1)$$

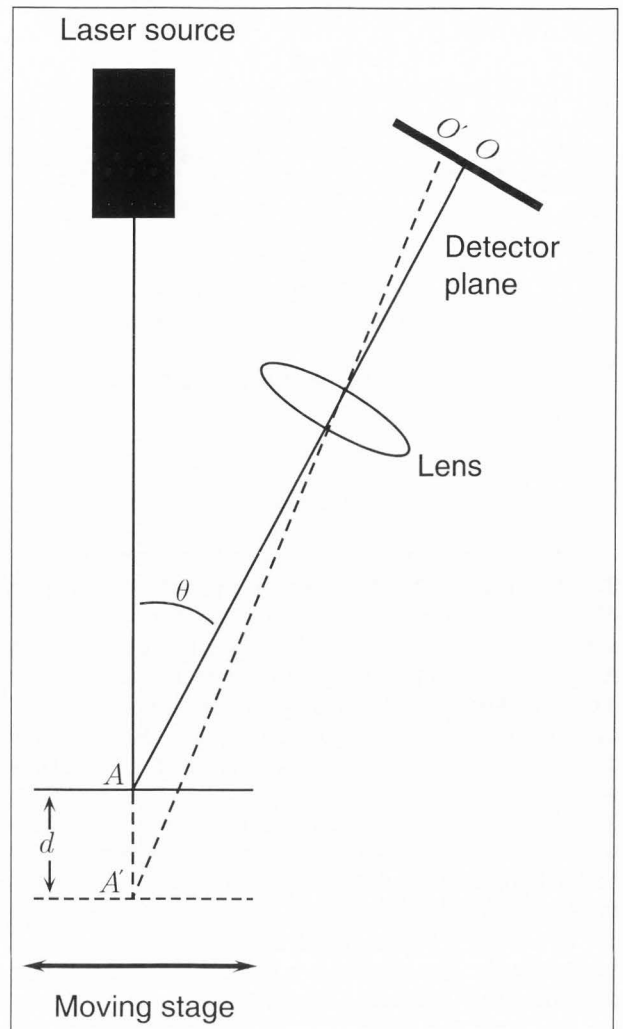


Figure 1. Schematic view of the triangulation process involved in the determination of surface coordinates.

where  $m$  is the magnification of the detector focusing lens and  $OO'$  is the distance between the two images. The focused laser beam is scanned over the surface to be inspected while its image position is recorded by the camera. The  $x:y$  position of the spot image for each step of the moving stage and the distance of a reference plane surface from the camera are known. Differences of the recorded image surface position with respect to the reference plane thus allow evaluation of distance  $d$  of the surface from the reference plane in such a position (Cielo, 1988; p. 295). Proper signal-processing techniques build the three-dimensional model  $z(x, y)$  from  $x:y$  coordinates and the depth  $d$  (Laurendeau and Poussart, 1986; Chi, 1986).

Table 1. Surface fractal dimension of renal cystine stone fragments determined by the variation method. The second column gives the estimated fractal dimension ( $D_e$ ) while the third column gives the coefficient of correlation for the regression.

Sample Name	$D_e$	Corr. Coeff.
CA15_LZ1	2.16	0.9995
CA01_LZ1	2.32	0.9999
CA4BLZ1	2.45	0.9987

#### Data analysis

The data obtained are analyzed by the fractal geometry approach (Mandelbrot, 1982). The fractal dimension of surface  $S$  is a number between 2 and 3 which characterizes the space-filling property of the object (Pentland, 1985). The smoother the object, the closer the fractal dimension will be to 2, as opposed to a very convoluted surface with lots of sharp peaks and valleys, which will have a fractal dimension closer to 3. This is why fractal dimension correlates with the roughness of an object. Moreover it has already been shown that it describes surface texture in more detail than conventional roughness parameters (Chesters et al., 1989) and that it has a relationship to fracture toughness (Mecholsky et al., 1989).

In this study, the fractal dimension was determined by the variation method developed by Dubuc et al. (1989). Surface  $S$ , composed of numerous peaks and valleys, is dilated by a horizontal segment of length  $2\epsilon$  to give  $S_\epsilon$  (the approximation of  $S$  at scale  $\epsilon$ ). Then, volume  $V(S_\epsilon)$  of this dilated object is calculated. It is the growth rate of  $V(S_\epsilon)$  when  $\epsilon$  tends to 0 that is related to the fractal dimension of the object. In fact, the relationship is:

$$D = \lim_{\epsilon \rightarrow 0} \left[ 3 - \frac{\log V(S_\epsilon)}{\log \epsilon} \right] \quad (2)$$

where  $D$  is the surface fractal dimension. In practice, however,  $D$  is obtained through the graph of  $\log(1/\epsilon)$  as a function of  $\log [V(S_\epsilon)/\epsilon^3]$ . When  $\epsilon$  is appropriate, this diagram yields a straight line relationship and the slope of the best line fit ( $D_e$ ) is the fractal dimension of the surface. The variation method is a technique for obtaining the log-log data for a surface in an efficient and accurate manner and has the property of being invariant to scale and translation. A detailed mathematical and computational description of the algorithm is found elsewhere (Dubuc et al., 1989).

#### Results and Discussion

Figures 2A-C show the surface of cystine stones fragments at low magnification. These samples are composed of cystine at a concentration greater than 91%

P/P and they exhibit a markedly different texture. In a qualitative description, while the sample in Figure 2A appears relatively smooth, the sample in Figure 2C is definitely rough. These fragments clearly reveal progressive roughness at a higher level of magnification [Figures 3A-C]. Variations in the texture of these stones may be caused by several factors, including size/shape characteristics of the building units, packing and consolidation conditions, and the nature of the adhesive material between crystallites.

Regions of 12 mm by 14 mm were scanned. The stone fragments had a diameter varying between 6 and 10 mm. The lateral resolution was 31  $\mu\text{m}$  in the horizontal and 25  $\mu\text{m}$  in the vertical direction. The depth of view was 2.5 mm while the laser spot size was approximately 50  $\mu\text{m}$ . In all cases the reference plane was set to be the lowest point with respect to the scanned object (note that this is irrelevant since the variation method is translation invariant). The calibration for such an apparatus was delicate but was done at the beginning of the data acquisition and stayed the same for all samples. Plots of the reconstructed 3D signal,  $z(x, y)$ , for the different samples are shown in Figure 4.

The variation method has been applied to user-defined regions on the sampled data. Typical log-log plots are shown on Figure 5 while actual estimation results for each sample are given in Table 1. For all calculations  $\epsilon$  was varying between 100  $\mu\text{m}$  and 1000  $\mu\text{m}$ , the lowest possible cutoff scale being limited by the resolution of the data. Observe that the fractal dimension correlates well with our qualitative assessment of roughness for the three samples. The fractal dimension of the surface can therefore be used to quantify the degree of irregularity of the surface created by the contribution of the variables mentioned earlier and the results of their interactions.

#### Limitations of the technique

The data acquisition has some limitations that should be pointed out. First, the surface sampling with triangulation needs the surface of the scanned object to be convex. 3D measurements may be obtained only for those surface portions accessible simultaneously by the laser source and the camera line of sight. Many surface portions of rough surfaces or concave surfaces are thus inaccessible. One solution would be to select multiple views of the same object at different orientations and to reconstruct the object by fusing the views. Although this would improve the situation slightly, some surface portions would always remain inaccessible.

Second, there are limitations in both the spatial ( $x:y$ ) and depth ( $d$ ) resolutions. Getting the best possible measurements of the 3D surface geometry is not the goal of this project, however to increase spatial resolution, other techniques such as depth-from-focus, scanning tunneling microscopy or coherence radar (Dresel et al., 1992) could be used for surface characterization. These meth-

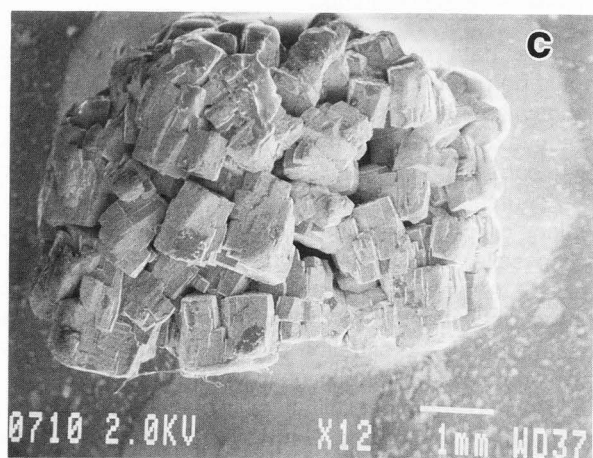
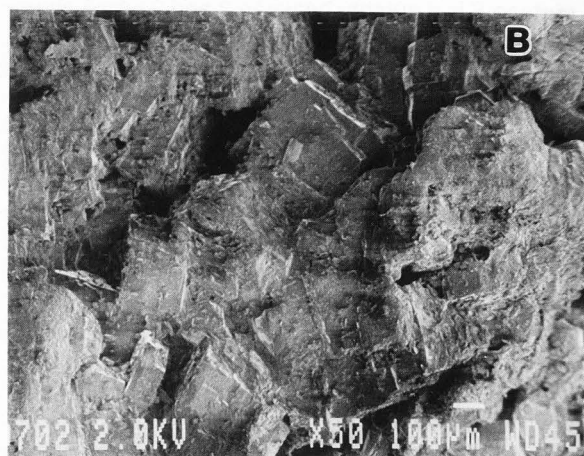
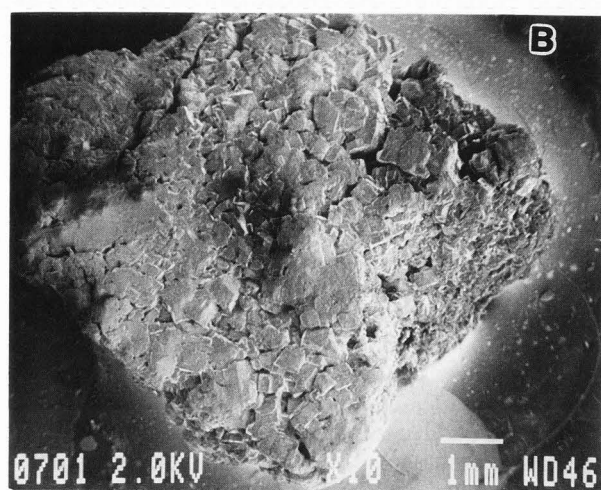
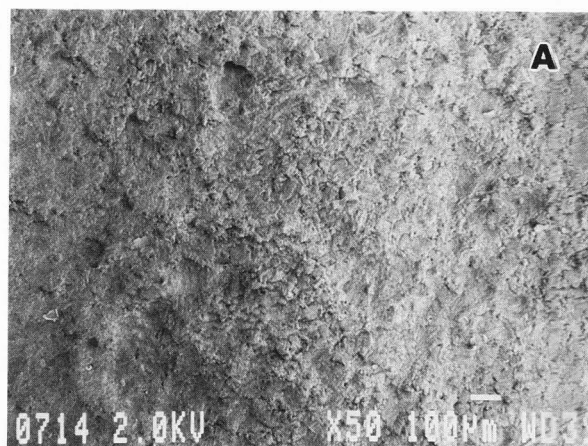
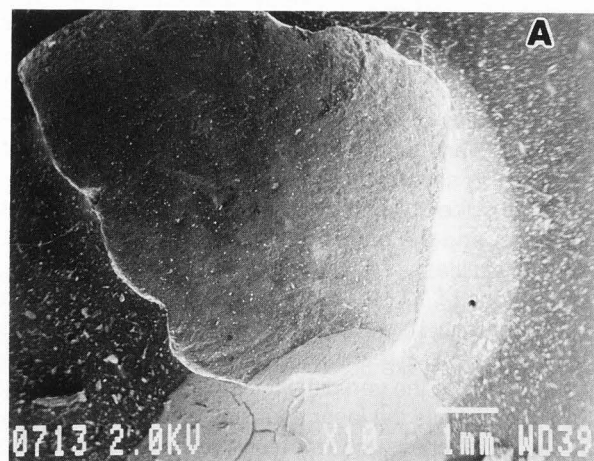


Figure 2. External surface of renal cystine stone fragments at low magnification: (A) CA15.LZ1; (B) CA01.LZ1; (C) CA04BLZ1.

Figure 3. External surface of renal cystine stone fragments at high magnification: (A) CA15.LZ1; (B) CA01.LZ1; (C) CA04BLZ1.

Surface Roughness Evaluation of Cystine Stones

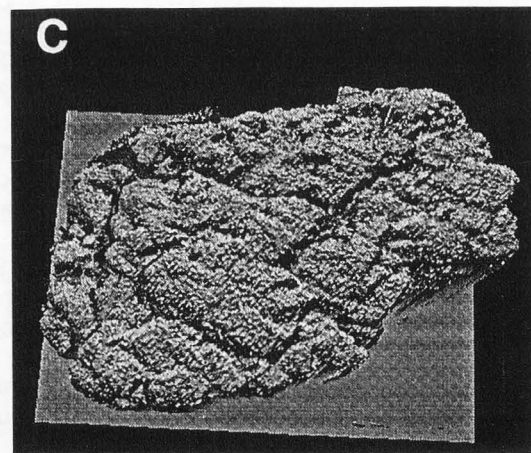
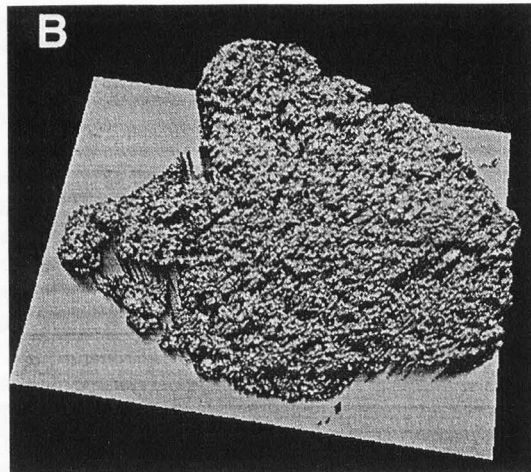
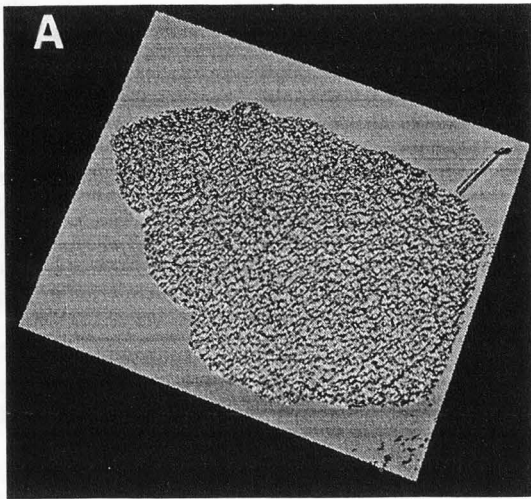


Figure 4. Rendered version of the depth map  $z(x, y)$  for the different samples. (A) CA15.LZ1; (B) CA01.LZ1; (C) CA04BLZ1.

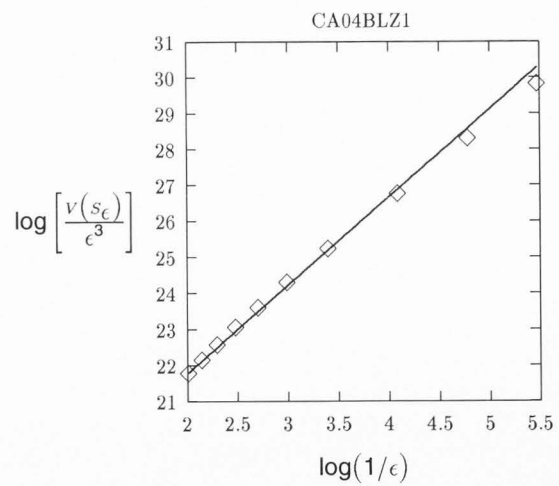
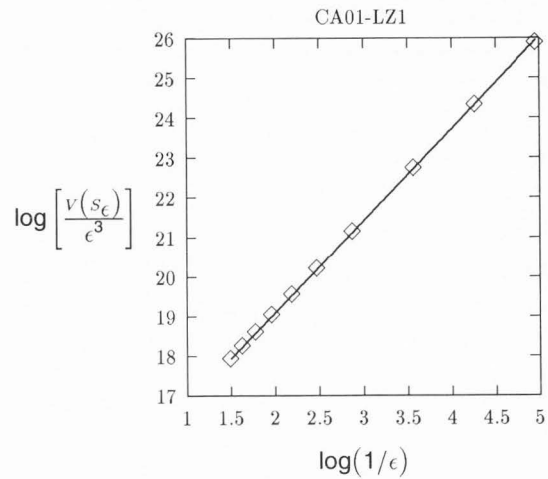
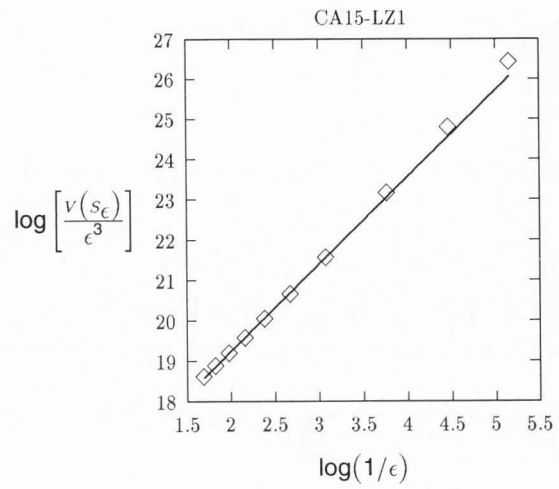


Figure 5. Log-log plots used to determine surface fractal dimension. Top: CA15.LZ1; Middle: CA01.LZ1; Bottom: CA04BLZ1.

ods will suffer from other limitations such as depth-of-view or sampled surface size. This then suggests the need to be able to fuse data obtained at different scales from different sensing devices.

As far as the data analysis is concerned, the precision of the estimated fractal dimension is bound to the resolution of the data available and to the actual fractal dimension of the object. The smoother an object is, the easier it will be to obtain a good precision in the estimation. In this study, we were not concerned by the absolute precision of the computed data but rather in the relative difference of the estimates from one sample to the next. Finally it is important to note that in this application the estimated fractal dimension is only valid within the range of scales studied.

### Conclusions

The method presented here to evaluate the surface roughness of cystine fragments decidedly offers a valuable, flexible, and non-destructive quantitative approach that goes beyond rank order classification. It provides a tool for the study of physical and chemical processes at interfaces. The application of such a technique could provide a framework for testing and extrapolating the detailed texture of bioactive materials and biological surfaces. In addition, it could provide an ideal opportunity to investigate and characterize the mechanisms of 1) fragmentation and 2) bioadhesion.

### Acknowledgements

The technical assistance of Laboratoire CM2 (École Polytechnique, Montréal, PQ) is gratefully acknowledged. The authors thank Dr M. Hassouna (Royal Victoria Hospital, Montréal, PQ) and Dr D. Fletcher (Louis C. Herring & Co., Orlando, FL) for providing cystine stone samples studied. Fonds FCAR (R. Thibert), J. H. Stewart-Reid Memorial Foundation (B. Dubuc) and MRC support is acknowledged.

### References

- Avnir D, Farin D (1990). Fractal Scaling Laws in Heterogeneous Chemistry. Part 1: Adsorption, Chemisorption and Interactions Between Adsorbates. *New J. Chem.*, **14**, 197-206.
- Bhatta KM, Prien EL, Drettler SP (1989). Cystine Calculi - Rough and Smooth: A New Clinical Distinction. *J. Urol.*, **142**, 937-940.
- Brunette DM (1988). The Effect of Surface Topography on Cell Migration and Adhesion. In: Ratner BD, Editor. *Surface Characterization of Biomaterials*. Elsevier, New York, p. 203-217.
- Chesters S, Yen HY, Lundin M, Kasper G (1989). Fractal-based Characterization of Surface Texture. *Applied Surface Science*, **40**, 185-192.
- Chi ZC (1986). Recognition for 3-D Surface Shape Using Multiple Distance Feature. In: Cielo P, Editor. *Optical Techniques for Industrial Inspection*. Proc. SPIE, **665**, p. 217 (abstract).
- Cielo P (1988). *Optical Techniques for Industrial Inspection*. Academic Press, San Diego.
- Dickson LD, Harkness D (1969). *Surveying and Tracking Instruments*. In: *Applied Optics and Optical Engineering*. Kingslake R, Editor. Academic Press, New York, 1969, p. 231.
- Dresel T, Hausler G, Venzke H (1992). Three-dimensional sensing of rough surfaces by coherence radar. *Applied Optics*, **317**, 919-925.
- Dubuc B, Zucker SW, Tricot C, Wehbi D, Quiniou JF (1989). Evaluating the Fractal Dimension of Surfaces. *Proc. Roy. Soc. (London Series A): Math. Phys. Sci.*, **425(1868)**, 113-127.
- Dufour M, Bégin G (1984). Adaptive Robotic Welding Using a Rapid Image Pre-processor. Proc. SPIE, **449(P1)**, 338-345.
- Fowler SA, Gaertner KL (1990). Scanning Electron Microscopy of Deposits Remaining in Soft Contact Lens Polishing Marks After Cleaning. *Ciao J.*, **16(3)**, 214-218.
- Hess H (1978). Tablets Under the Microscope. *Pharm. Technol.*, **2**, 36-43.
- Laurendeau D, Poussart D (1986). Unsupervised Model Building of 3-D Objects Using Range Information. In: Cielo P, Editor. *Optical Techniques for Industrial Inspection*. Proc. SPIE, **665**, p.209.
- Mandelbrot BB (1982). *The Fractal Geometry of Nature*. W.H. Freeman, San Francisco, p 14-19, C8-C15.
- Mecholsky JJ, Passoja DE, Feinberg-Ringel KS (1989). Quantitative Analysis of Brittle Fracture Surfaces Using Fractal Geometry. *J. Am. Ceram. Soc.*, **72(1)**, 60-65.
- Merritt K, Chang CC (1991). Factors Influencing Bacterial Adherence to Biomaterials. *J. Biomat. Applic.*, **5(3)**, 185-203.
- Pentland AP (1985). On Describing Complex Surface Shapes. *Image and Vision Computing*, **3(4)**, 153-162.
- Rowe RC (1978). The Measurement of the Adhesion of Film Coatings to Tablet Surfaces: The Effect of Tablet Porosity, Surface Roughness and Film Thickness. *J. Pharm. Pharmacol.*, **30**, 343-346.
- Thibert R, Tawashi R (1991). The Study of the Surface Geometry of Renal Stone Fragments After Shock Wave and Ultrasound Disintegration. *Scanning Microsc.*, **5**, 549-554.
- Trudelle F, Rowe RC, Witkowski AR (1988). Monitoring Production Scale Film Coating Using Surface Roughness Measurements. *S.T.P. Pharma*, **4(1)**, 28-30.
- Zografis G, Johnson JA (1984). Effects of Surface Roughness on Advancing and Receding Contact Angles. *Int. J. Pharm.*, **22**, 159-176.

Discussion with Reviewers

T. J. Mackin: What is the spot size of the laser, and how does this affect the horizontal and vertical resolution of the technique?

Authors: The spot size of the laser was approximately 50  $\mu\text{m}$  in diameter. The spot size is limited by diffraction and is determined by the projection lens aperture. The depth of field is also determined by the lens aperture. The minimum spot size is given by:

$$W_2 = \frac{2\lambda F}{\pi W_1}$$

and the depth of focus (*DOF*) is given by

$$DOF = \frac{8\lambda}{\pi} \left( \frac{F}{W_1} \right)^2$$

where  $W_1$  is the input beam diameter,  $\lambda$  is the laser wavelength and  $F$  the lens focal length. The 50  $\mu\text{m}$  size was selected as a good compromise between horizontal resolution and depth of field (2.5  $\text{mm}$ ).

T. J. Mackin: Does the experimentalist have the option of rotating the object (or detector) to get a complete mapping of the surface, or does one choose to map only a small portion of the surface?

Authors: Four orthogonal views of each sample were taken. These were obtained by rotating the samples. For the analysis, we chose only one view per sample (the left view) and selected regions on the reconstructed surfaces for the estimation of the fractal dimension. We did not attempt to fuse the views since the results with one view were acceptable.

X. Maldagne: It is well known that speckle appears when a monochromatic source such as a laser beam is used for the illumination of a "rough surface". How does this speckle affect the measurements, especially for micro-roughness measurements?

Authors: The speckle size within the imaging plane of the detector resulting from coherent illumination at  $\lambda = 0.8 \mu\text{m}$  of a rough surface will be in the range of the  $F$ -number of the camera lens (Cielo, 1988; pp. 181-182). The average number of speckle grains collected by a CCD element of the camera imaging plane will be

$$N \simeq \left( \frac{a_d}{2d} \right)^2$$

where  $a_d$  is the diameter of the CCD element and  $2d$  is the average center-to-center distance between speckle grains. The resulting signal-to-noise ratio (*SNR*) will be

$$SNR = N^{1/2}$$

For a CCD element diameter of 25  $\mu\text{m}$  and a lens  $F$ -number of 8, the *SNR* is in the range of 3. In practice, it means that the accuracy of the range sensor can hardly be pushed to subpixel values when dealing with rough surfaces and that it is rather related to the size of the laser spot image on the camera detector plane. However, the laser range sensor was required to measure large surface features from 100  $\mu\text{m}$  up to 1  $\text{mm}$  which is much larger than microtexture features and thus the measurements usefulness was not compromised by speckle noise.

X. Maldagne: Cystine renal stones, why such particular stones, any reason? Why coat them with 100 Å carbon fiber?

Authors: Cystine stones were selected as a model of renal stones and because the surface roughness of these stones has been associated with the stone hardness and resistance to fragmentation.

The coating of the stones is due to the fact that the sample surfaces are partially translucent. Part of the light would be transmitted under the surface and rediffused to the camera from an area larger than the one directly illuminated by the laser source. Such an effect limits the vertical and horizontal resolution of the measurements. The carbon coating limits the amount of light transmitted under the surface and improves the resolution.

J. J. Mecholsky: The authors refer to a "roughness-fragmentation" relationship in the paper. However, they do not specify what that relationship is. Presumably, the fragmentation increases with increasing roughness. The authors should specify this, if they are able.

Authors: The exact relationship is not known, however the establishment of a quantitative method to assess surface roughness in 3D using fractal geometry will set the stage for determining the exact relationship between roughness and fragmentation.

C. Roques-Carnes: Any log-log representation does not necessarily refer to the fractal concept.

Authors: The variation method assumes that the graph of the function to be studied has a predominant vertical tendency and this is mostly verified in the case of rough surfaces. The  $\epsilon$ -variation is the volume of the Minkowski addition of an  $\epsilon$ -square to the graph of a function. It is the rate of growth of this volume that is used to characterize the complexity of the studied object (this object being 'fractal' or not). Transposing in log-log space allows us to assess the dominating tendency.